Biogeosciences Discuss., https://doi.org/10.5194/bg-2018-195
Manuscript under review for journal Biogeosciences
Discussion started: 3 May 2018
© Author(s) 2018. CC BY 4.0 License.

Biogeosciences Discussions
Open Access
EGU

Seasonal and spatial variability of methane emissions from a subtropical reservoir in Eastern China

Yang Le*, Li Hepeng, Yue Chunlei, Wang Jun

Zhejiang Academy of Forestry, Hangzhou, 310023, China

Corresponding author: *E-mail: yangboshi@live.cn

Biogeosciences Discuss., https://doi.org/10.5194/bg-2018-195
Manuscript under review for journal Biogeosciences
Discussion started: 3 May 2018
© Author(s) 2018. CC BY 4.0 License.

Abstract:

Subtropical reservoirs are important source of atmospheric methane (CH_4). This study aims to investigate the spatiotemporal variability of CH_4 emission, using the methods of static floating chambers and bubble traps, from the water surfaces of Xin'anjiang Reservoir. Seasonal variability showed that CH_4 emission from the main reservoir body was high in autumn and low in spring, with medium values in summer and winter. The dynamics of CH_4 emission was flat from February to June, but fluctuated dramatically from July to January in the upstream river, which was interrupted by the bubbles in the second half year. However, CH_4 emission was largely influenced by the streamflow in the downstream river, with a minimum value in February due to an extreme low streamflow (275 $m^3\ s^{-1}$). Spatial variability showed the upstream river had the highest CH_4 flux (3.90 ± 7.80 mg $CH_4 \cdot m^{-2} \cdot h^{-1}$), followed by the downstream river (0.50 ± 0.41 mg $CH_4 \cdot m^{-2} \cdot h^{-1}$), and the main reservoir body stood the last place (0.01 ± 0.07 mg $CH_4 \cdot m^{-2} \cdot h^{-1}$). Therefore, it was necessary to capture the variation of CH_4 emission from reservoirs in the space and time scales to avoid the error of estimating the CH_4 emission incorrectly.

Key words: Spatiotemporal variability; CH_4 flux; CH_4 emission; Bubble; Xin'anjiang Reservoir.

Biogeosciences Discuss., https://doi.org/10.5194/bg-2018-195
Manuscript under review for journal Biogeosciences
Discussion started: 3 May 2018
© Author(s) 2018. CC BY 4.0 License.

1. Introduction

Reservoirs are an important type of wetland, which used to be often regarded as clean energy. However, the view was denied by a growing body of researches documenting their role as carbon sources. Deemer et al. (2016) showed that CH_4 emissions are responsible for the majority of the radiative forcing from reservoir water surfaces (approximately 80% over the 100-year timescale). The greenhouse gas emission data was limited to 36 Asian reservoirs, among which CH_4 emission flux data was available in 3 reservoirs in China, *i.e.*, Three Gorges (Yang et al., 2013; Zhao et al., 2013), Ertan (Zheng et al., 2011), Miyun (Yang et al., 2014). Actually, China had 98,002 dams of different sizes with 142 large-size hydroelectric reservoirs, which did not include the dams under construction or planed now. Thus, more hydroelectric reservoirs distributed in the different geographical regions and climate zones in China should be selected to measure CH_4 emission flux to explore the rules of CH_4 emission from hydroelectric reservoirs.

Diffusive flux, gas bubble flux, and aquatic vegetation are main pathways for CH_4 emission from open water areas in reservoirs (Bastviken et al., 2011). Plant-medium transport is an important CH_4 emission pathway in reservoir area with abundant vegetation cover (Bastviken et al., 2011). However, in the no vegetation-distributed areas, ebullition was a dominant way for CH_4 emission, while molecular diffusion was a secondary way for CH_4 emission from the reservoir water surfaces, although ebullition was found to be episodic (Maeck et al., 2014), because the ebullitive CH_4 flux was larger by 1~3 orders of magnitude than the diffusive CH_4 flux (Delsontro et al., 2010, 2011). High ebullitive CH_4 flux was often observed in the shallow zones, river deltas, and inflow rivers (Delsontro et al., 2010, 2011, 2016), which was influenced by allochthonous organic carbon input and burial (Sobek et al., 2012). Chamber methods were used to measure the CH_4 emission flux in the previous studies located in the 3 reservoirs in China, and chamber methods measured the total CH_4 emission flux (diffusion plus ebullition) across water-air interface (Yang et al., 2013, 2014; Zheng et al., 2011; Zhao et al., 2013). Probably these previous studies didn't

© Author(s) 2018. CC BY 4.0 License.

show the bubble CH_4 flux magnitude.

Spatial and temporal variability in CH_4 emission are often reported in the reservoirs (Yang et al., 2013; Zhao et al., 2013; Zheng et al., 2011; Muzenze et al., 2014). The spatial variability in CH_4 emission from reservoirs are caused by the impoundment of the dams, which changed the hydrological characteristics of the original river. Upstream and downstream of the dams, outlet of the dam, and inflow rivers to the reservoirs had distinct CH_4 emission levels in a whole reservoir's system (Muzenze et al., 2014; Kemenes et al., 2007; Abril et al., 2005), because of the hydrological variables (e.g., water velocity, water depth) (Yang et al., 2013) and dam operation strategy (Fearnside and Pueyo, 2012). Turning to the temporal variability in CH_4 emission, temperature, water column mixing, dissolved oxygen (DO) concentration and other environmental variables (e.g., retention time, benthic metabolism) controlled the temporal variability in CH_4 emission (Yang et al., 2013; Natchimuthu et al., 2016; Rodriguez and Casper, 2018). For example, CH_4 emission reached the maximum in the summer and turned to the low levels in the other seasons in the Three Gorges Reservoir, which was regulated by temperature, DO, and water velocity (Yang et al., 2013). Temperature regulated the temporal variability of CH_4 emission in the 3 lakes (Följesjön, Erssjön, Skottenesjön) of southwest Sweden (Natchimuthu et al., 2016). Due to the differences in hydrology, water quality, meteorological, and biological variables, the spatiotemporal variability in CH_4 emission should be explored in the reservoirs, which could understand the differences of CH_4 emission in time and space scales.

Downstream rivers also cannot be ignored because of the degassing fluxes at the turbines or spillways and high fluxes in the downstream watercourses. Downstream emission accounted for 50% of total CH_4 emissions from the Balbina Reservoir in Brazil (Kemenes et al., 2007), roughly 30% of total greenhouse gas emissions for the 8 reservoirs in the dry tropical biomes region in Brazil (Ometto et al., 2013), and 10% of total CH_4 emission for Nam Theum 2 Reservoir in Laos (Deshmukh et al., 2016).

Biogeosciences Discuss., https://doi.org/10.5194/bg-2018-195
Manuscript under review for journal Biogeosciences
Discussion started: 3 May 2018
© Author(s) 2018. CC BY 4.0 License.

Therefore, CH_4 emission from the downstream river should be included in a hydroelectric reservoir.

Two hypothesis are postulated here: (1) the temporal variations in CH_4 emission from water surface are influenced by the temperature, thus a high CH_4 emission flux would be observed in summer and relative low CH_4 emission fluxes occurred in other seasons; (2) upstream and downstream rivers have a great CH_4 emission because of the fast water flow and the low water depth there. The specific objectives in this study are to investigate the temporal variations in CH_4 emission from Xin'anjiang Reservoir, and upstream and downstream sites are contrasted with those in the reservoir to show the spatial variations in CH_4 emission from the reservoir.

2. Materials and Methods

2.1. Study sites

Figure 1. Dynamics of precipitation, evaporation, air temperature, and water level in the Xin'anjiang Reservoir region

Xin'anjiang Reservoir (29°28'-29°58'N, 118°42'-118°59'E) is located in the north subtropical zone, with the mean air temperature of 17.7 °C, the total precipitation of 2015.1 mm, and the total evaporation of 712.9 mm (Figure 1). Xin'anjiang Reservoir was built in 1959, which has a water area of 567 km^2, a mean depth of 34 m. The water storage of the reservoir is about 1.78×10^{10} m^3, the yearly average inflow and the outflow discharge are 9.4×10^9 m^3 and 9.1×10^9 m^3, respectively, and the water retention time is about 2 years (Li et al., 2011). Water level fluctuated between 98m to 104m in Xin'anjiang Reservoir in 2015 (Figure 1). The Xin'anjiang Reservoir is dendritic shape, which consists of northwest lake, northeast lake, southwest lake, southeast lake, and central lake (Figure 2). Among the 5 sub-lakes, the watercourse of northwest lake is the most dominant upstream inflow river, which occupy 60~80% of total surface runoff. Thus, the northwest lake is regarded as the main upstream river of the Xin'anjiang Reservoir, and the reservoir's main body consisted of northeast lake,

© Author(s) 2018. CC BY 4.0 License.

southwest lake, southeast lake, and central lake, and the downstream river is the watercourse below the Xin'anjiang Dam.

Figure 2. The distribution of the sampling transects and sampling sites in the Xin'anjiang Reservoir

The sampling campaign was conducted in the 4 sub-lakes and the downstream river (Figure 2). The northwest (NW) lake transect (29°44'03" N, 118°43'04" E) was located in Jiekou town of Anhui Province, where was the main inflow inlet of Xin'anjiang Reservoir and had a width of 0.3 km. 3 sampling points (NWP1, NWP2, NWP3) were chosen from the margin to pelagic zones in the NW transect. The northeast (NE) lake transect (29°38'44"N, 119°03'03"E) was located in open water areas of the NE lake near the outlet of a tributary (Jinxianxi). The southwest (SW) lake transect (29°28'18"N, 118°44'39"E) was located in the open water areas near Maotoujian Island, where was outlet of the Jiangjia tributary and Fengkou tributary. The southeast lake (SE) transect (29°28'39"N, 118°45'20"E) was located in the open water areas between Guihua Island and Mishan Island, where was about 5 km upstream of the Xin'anjiang Dam. 5 sampling points (from P1 to P5) were chosen from the margin to pelagic zones in the NE, SW, and SE transects, respectively. In addition, 4 sampling points were selected in the downstream river below the dam, with a distance of 0.35 km, 1 km, 4 km, and 7 km away from the Xin'anjiang Dam, respectively, which was named as DRP1, DRP2, DRP3, and DRP4, respectively.

2.2. CH_4 flux measurements

In this study, the floating static chambers were used to collect CH_4 gas samples from the surface of Xin'anjiang Reservoir from December 2014 to December 2015. Monthly measurement was carried out for each sampling site in the morning, and the measurement lasted for half an hour for each point. The bubble traps were used to collect the bubbles in the upstream river from August 2016 to November 2017. The bubbles were collected once or twice in the NW transect every month except November, 2016, January and February, 2017, and the collection campaign often

Biogeosciences Discuss., https://doi.org/10.5194/bg-2018-195
Manuscript under review for journal Biogeosciences
Discussion started: 3 May 2018
© Author(s) 2018. CC BY 4.0 License.

lasted for about 1 day.

The diffusive CH_4 emission flux was measured using the static chamber and gas chromatograph method. The floating static chamber (0.29 m^2 for the basal area; 0.117 m^3 for the volume) consisted of a plastic box without a cover that was wrapped in light-reflecting and heatproof materials to prevent temperature variation inside the chambers; in addition, plastic foam collars were fixed onto opposite sides of the chamber. The headspace height inside the chamber was about 35 cm. A silicone tube (0.6 cm and 0.4 cm outer and inner diameters, respectively) was inserted into the upper central side of the chamber to collect gas samples, and the gas samples were dried with plexiglass tubes filled with Calcium chloride anhydrous (analytical reagent), which could remove the moisture in the gas samples and prevent the biological reactions. Another silicone tube was inserted into the upper corner side of the chamber to keep the air pressure balanced between the inside and the outside of the chamber. All measurements were performed in triplicate. The gases in the headspace of the chamber were collected into air-sampling bags (0.5L; Hedetech, Dalian, China) four times every 7 min over a 21 min period using a hand-driven pump (NMP830KNDC; KNF Group, Freiburg, German) (Yang et al., 2013). Once the gas was collected from the chambers, the gas samples were stored in the air-sampling bags until analysis in the laboratory. The air-sampling bags made of aluminum can store the gas samples for 7 days, which does not absorb and react with CH_4. The leakage and memory effects of air-sampling bags have been tested before our experiments.

The bubble trap consisted of an inverted 30 cm diameter circular funnel fixed with a closed plastic bottle (volume: 0.56 L) in its narrow neck, and an additional skirt (50 cm diameter circular) was fixed in the large mouth of the funnel to enlarge the bubble collection range (Wik et al., 2013). Each funnel was stabilized by three equally sized weights to make sure no tiny bubbles left in the bottles at initial stage. 16 to 26 bubble traps were fixed in a river-crossing rope with a distance of about 10-15 m between the

© Author(s) 2018. CC BY 4.0 License.

two neighbouring bubble traps when the bubbles were sampled. The trapped gas bubbles would drain the water from the bottles after about 20-40 hours placement. The left water in the bottles was measured by a graduate to calculate the volume of trapped gas bubbles. The trapped gas was diluted 1000 times by injecting 1 mL trapped gas into 1 L or 0.5 L previously N_2-filled gas bags, because the CH_4 concentration of the trapped gas was too high for the gas chromatograph to reach.

The air-sampling bags were analyzed within 3 days using a gas chromatograph (Agilent 7890A; Agilent Technologies, Santa Clara, USA) equipped with a flame ionization detector (FID) and separated with a Teflon column (3 m × 3 mm) packed with Porpak-Q column (80-100 mesh). The oven, injector, and detector temperatures were at 70 °C, 25 °C, and 200 °C, respectively. The flow rate of the carrier gas (N_2) was 25 mL·min^{-1}, and the flow rate of H_2 and the compressed air was set to 40 and 30 mL·min^{-1}, respectively. Standard mixed gas (CH_4: 1.83 ppm; provided by China National Research Center for Certified Reference Materials, Beijing) was used to quantified the CH_4 concentration in one of every 10 samples, which kept the coefficient of variation of the CH_4 concentration in the replicated samples below 1%.

The increasing rate of the gas concentration (dc/dt) within the static chamber was calculated as the slope of the linear regression of the gas concentration versus time. It was suggested that the nonlinear relation between gas flux and time would be better to determine the steeper initial slope in the chambers. If one plots the time rate of change of concentration in a closed box, it will be curvilinear, so if measurements were made at successive time steps, a parabola regression was fit to the data and the slope at time zero detected (Hutchinson and Livingston, 2001). Thus, the para-curve model was made preferentially than the linear one. Otherwise, the linear model was accepted. Acceptance of the results was based upon two criteria: (1) The difference of CH_4 concentration between the initial gas sample and ambient air must be within 10% and (2) the correlation coefficient (R^2) had to be > 0.90.

Biogeosciences Discuss., https://doi.org/10.5194/bg-2018-195
Manuscript under review for journal Biogeosciences
Discussion started: 3 May 2018
© Author(s) 2018. CC BY 4.0 License.

$$F_1 = \rho \times \frac{dc}{dt} \times \frac{273.15}{273.15+T} \times H \quad (1)$$

where F_1: the diffusive CH_4 flux (mg $CH_4 \cdot m^{-2} \cdot h^{-1}$); ρ: density of gas under the standard conditions (0.714 $kg \cdot m^{-3}$ for CH_4); H: height of the top of the inverted chamber to the water surface (0.35 m here); 273.15: absolute temperature at 0 °C; T: air temperate (°C).

Actually, the static floating chambers can collect both of diffusive and bubble CH_4 emission fluxes. Bubbles caused the CH_4 concentrations pulses in these chambers. The average CH_4 emission fluxes (F_a; mg CH_4 m^{-2} h^{-1}) in the transects were calculated by the following equation (2)

$$F_a = \frac{\sum_{n=1}^{n=13} \left[\frac{\sum_{m=1}^{m=5} \left(\frac{\sum_{i=1}^{i=3} F_m}{i} \right)}{m} \right]}{n} \quad (2)$$

Where, i: the numbers of chambers (3 chambers here); m: the sampling stations in the transect (NW: 3; NE, SW, SE: 5; DR: 4); n: the total measurement times of CH_4 emission during the given time (total times of 13 in 2015, See Table S.1, S.3-6); F_m: the measured CH_4 emission flux by the floating chambers.

The mass flux of CH_4 via ebullition (bubble CH_4 flux) is

$$F_2 = \frac{C_{CH4} \times V \times M}{A_f \times t \times V_m} \quad (3)$$

Where F_2: the ebullitive CH_4 flux (mg $CH_4 \cdot m^{-2} \cdot h^{-1}$); C_{CH4}: CH_4 concentration ($\mu L \cdot L^{-1}$); V: the accumulated headspace gas volume (L); M: molar weight of CH_4 (16.04 $g \cdot mol^{-1}$); A_f: the funnel area (0.14 m^2); t: the fractional number of hours between measurement; V_m: the molar volume of gas at standard conditions (22.4 $L \cdot mol^{-1}$; gas samples equilibrated to room temperature before analysis) (Wik et al., 2011).

The ebullition rate (ER; ml m^{-2} h^{-1}) reflected the speed of accumulated volume of

Biogeosciences Discuss., https://doi.org/10.5194/bg-2018-195
Manuscript under review for journal Biogeosciences
Discussion started: 3 May 2018
© Author(s) 2018. CC BY 4.0 License.

bubbles released from the water surface, which was calculated by the following equation (4).

$$ER = \frac{V}{A_f \times t} \quad (4)$$

The parameters of V, A_f, and t are given in equation (3).

2.3. Statistical Analysis

The CH_4 flux values were firstly tested by the Kolmogorov-Smirnov test to judge whether these data satisfied the normal distribution. If not, these CH_4 flux data would be transferred by the trigonometric function or logarithmic function to satisfy the normal distribution. Then one-way analysis of variance (ANOVA) combined with Tukey HSD test was used to analyze the seasonal and spatial variability in CH_4 emission flux. The data were analyzed using the SPSS (Statistical Product and Service Solution) 18.0 statistical package.

3. Results

3.1. Seasonal Variations in CH_4 Emission

Figure 3. Average CH_4 emission from the 3 sampling points in the NW transect of the Jiekou town between Dec. 2014 to Jan. 2016
Note: NWP1, NWP2, and NWP3 have a distance of about 10 m, 50 m, and 120 m to the south bank, respectively.

CH_4 emission fluxes were measured by the static floating chambers in the upstream river in 2015, which included the ebullitive and diffusive CH_4 emission. The frequency of bubble occurrence was 16.2% in the NW transect during our measurement periods (Table S1). The CH_4 emission fluxes in the pelagic zones (NWP2 and NWP3) were significantly higher than those in the margin zone (NWP1), because no bubbles occurred in NWP1 (Figure 3). CH_4 emission from the pelagic zones was low from February to June, but increased and fluctuated significantly from July to January, while CH_4 emission from the margin zones always kept a low emission level during the measurement periods (Figure 3).

© Author(s) 2018. CC BY 4.0 License.

264

265 **Figure 4.** Dynamics of trap bubble flux, ebullition rate, and CH_4 concentration in the NW transect.
266 Note: The X axis of DOY, i.e., days of year, started from 3rd August, 2016

267

268 Ebullition rates, bubble CH_4 emission fluxes, and bubble CH_4 concentrations
269 measured using funnel-shaped gas traps in the NW transect, showed a similar
270 seasonal pattern with lower emissions in spring and higher emissions in summer and
271 autumn (Figure 4). Individual measurements ranged from 0 up to 150 mg $CH_4 \cdot m^{-2} \cdot h^{-1}$.
272 The mean bubble flux rate was 22.62 ± 15.07 mg $CH_4 \cdot m^{-2} \cdot h^{-1}$ in the NW transect,
273 ranging from 0.31 to 52.27 mg $CH_4 \cdot m^{-2} \cdot h^{-1}$. Measured CH_4 concentrations in the
274 collected gas ranged from 7.32 vol. % to 86.03 vol. % with a mean of 59.04 ± 23.27
275 vol. %. The average ebullition rate was 39.93 ± 24.28 $ml \cdot m^{-2} \cdot h^{-1}$, ranging from 1.17 to
276 76.39 $ml \cdot m^{-2} \cdot h^{-1}$. The ebullitive CH_4 flux had a significant positive correlated
277 relationship with the ebullition rate (R^2=0.92, $p<0.001$, Figure S1), and the bubble
278 CH_4 concentration (R^2= 0.76, $p<0.001$, Figure S2).

279

280 **Figure 5.** Dynamics of diffusive CH_4 emission from the 3 transects of reservoir's main body in
281 monthly scale.
282 Note: The different letters marked in the Fig. 5 indicated that the significant difference was found
283 in the 3 transects during the same sampling periods.
284
285 **Figure 6.** Seasonal variability of CH_4 emission from the 3 transects of reservoir's main body
286 Note: The different letters marked in the Fig. 6 indicated that the significant difference was found
287 in the NE transects among the different seasons.

288

289 The dynamic of average diffusive CH_4 fluxes fluctuated similarly among the 3
290 transects in the main body of the Xin'anjiang Reservoir, indicating a fluctuated
291 upwards pattern in 2015, with exception to one sudden peak in 1st August (DOY: 213),
292 and one slight peak between 20th January (DOY: 20) to 8th March (DOY:67) in the SW
293 lake (Figure 5). If CH_4 fluxes were analyzed by seasons, seasonal variations in CH_4
294 emission experienced a similar pattern in the NE, SW, and SE transects, which
295 climbed continuously from the minimum in the spring to the maximum in the autumn,
296 but decreased in the winter (Figure 6).

Biogeosciences Discuss., https://doi.org/10.5194/bg-2018-195
Manuscript under review for journal Biogeosciences
Discussion started: 3 May 2018
© Author(s) 2018. CC BY 4.0 License.

297

298 **Figure 7.** Dynamics of diffusive CH_4 emission from the downstream river.
299 Note: DRP1, DRP2, DRP3, and DRP4 has a distance of 0.35 km, 1 km, 4 km, and 7 km
300 downstream away from the Xin'anjiang Dam, respectively.

301

302 The average CH_4 flux experienced a similar seasonal variation pattern among the 4
303 sites in the downstream river (Figure 7): CH_4 flux decreased sharply from the
304 maximum value in January to the minimum value in February, and subsequently
305 fluctuated in a relatively small range (Figure 7).

306

307 *3.2. Spatial Variations in CH_4 Emission*

308

309 **Figure 8.** Average CH_4 emission from the different regions in the Xin'anjiang Reservoir.
310 Note: NW-B, bubble emission from the northwest transect; NW-D: diffusive emission from the
311 northwest transect; NE, northeast lake; SW, southwest lake; SE, southeast lake; DR, downstream
312 river. Different small letters represent the significant difference in average CH_4 emission flux
313 among the different transects at the level of p=0.05.

314

315 The average CH_4 emission flux was 3.90 ± 7.80 mg CH_4 m^{-2} h^{-1} in the NW transect
316 measured by the static floating chambers, including the bubble CH_4 flux (2.73 ± 2.02
317 mg CH_4 m^{-2} h^{-1}) and the diffusive CH_4 flux (1.17 ± 1.84 mg CH_4 m^{-2} h^{-1}; Figure 8). No
318 bubble CH_4 emission flux was found in the reservoir main body and the downstream
319 river by the method of the static floating chambers during the whole measurement
320 periods. The average diffusive CH_4 emission flux was 0.10 ± 0.07 mg CH_4 m^{-2} h^{-1} in
321 the main body of the reservoir. Specifically, the average diffusive CH_4 emission flux
322 was 0.090 ± 0.060 mg CH_4 m^{-2} h^{-1}, 0.13 ± 0.086 mg CH_4 m^{-2} h^{-1}, 0.079 ± 0.045 mg
323 CH_4 m^{-2} h^{-1} in the NE, SW, and SE transects, respectively (Figure 8). However, the
324 average diffusive CH_4 emission flux increased significantly in the downstream river
325 (DR: 0.50 ± 0.41 mg m^{-2} h^{-1}; Figure 8). The average diffusive CH_4 emission from the
326 main upstream river entrance (*i.e.*, NW transect) and the downstream river exceeded
327 that from the main body of the reservoir (*i.e.*, the NE, SW, and SE transects) by a
328 factor of 11 and 4, respectively (Figure 8).

329

© Author(s) 2018. CC BY 4.0 License.

Figure 9. Average CH_4 emission from the 4 sampling stations in the downstream river. Note: DRP1, DRP2, DRP3, and DRP4 has a distance of 0.5 km, 1 km, 4 km, and 7 km away from the Xin'anjiang Dam, respectively. Different small letters above the column indicate the significant difference among the 4 sites at the level of p=0.05.

No significant difference was found in CH_4 emission from the margin to pelagic zone of the 3 transects in the main body of reservoir. However, the average CH_4 emission flux decreased gradually in the downstream river with the distance to the Xin'anjiang Dam, with the maximum in DRP1 (0.83 ± 0.43 mg CH_4 m^{-2} h^{-1}) and the minimum in DRP4 (0.33 ± 0.25 mg CH_4 m^{-2} h^{-1}); the average CH_4 emission flux in the DRP1 was significantly higher than those of the other 3 sampling points in the downstream river ($p<0.001$; Figure 9).

4. Discussion

4.1. Seasonal Variations in CH_4 Emission

The dynamics of CH_4 emission from the upstream river were influenced by the interference of bubbles, and the peaks of CH_4 emission flux in Figure 3 were caused by bubbles (Table S1). In our study, bubbles occurred in the deep zone (>10 m) instead of the shallow zone (＜5 m), which was contrary to other studies (Rodriguez and Casper, 2018; Deshmukh et al., 2016). The high ebullitive CH_4 emission from the pelagic zone was probably related to the heterogeneity of sediment accumulation (DelSontro et al., 2010, 2011) while no or less sediment accumulation occurred along the margins of the reservoir (Mendonça et al., 2014).

The seasonal variability of CH_4 emission from the main body of Xin'anjiang Reservoir denied the hypothesis (1), because the maximum CH_4 emission occurred in autumn instead of summer in the 3 transects of the main body, although the significant difference of seasonal variability in CH_4 emission was only found in the NE lake (Figure 6). CH_4 fluxes had little relationship with air or water temperature after a linear correlated analysis. The explanation to the variability pattern of CH_4 emission flux in Figure 6 was probably related with the dynamics of DO concentration in the

© Author(s) 2018. CC BY 4.0 License.

water surface. Unfortunately, the DO values were not measured during our sampling campaigns. But a study on the dynamic distributions of DO in the 6 stations of Xin'anjiang Reservoir (3 stations overlap with this study) from Jan. 2011 and Dec. 2012 indicated that the maximum DO at surface layer was found in spring and the minimum value appeared in autumn, because phytoplankton started to breed in the proper temperature and light conditions at the surface layer in spring, which would release plenty of oxygen in the water column, while respiration overweight photosynthesis in autumn (Yin et al., 2014). The variability pattern of DO was contrary to the dynamics of CH_4 flux in Figure 6. CH_4 was mineralized to CO_2 by methanotrophic bacteria under aerobic water column (Schubert et al., 2012).

An obvious peak (0.25 ± 0.15 mg CH_4 m^{-2} h^{-1}) was observed in 1st August (DOY: 213) in the SW lake (Figure 5), and CH_4 fluxes in the two margin sampling points (i.e., SWP1 and SWP2) were 0.47 ± 0.11 mg CH_4 m^{-2} h^{-1} and 0.35 ± 0.081 mg CH_4 m^{-2} h^{-1}, respectively (Table S4), which had a large contribution to the CH_4 emission peak. The high CH_4 fluxes from the margin zone were likely attributed to the decomposed vegetation in the littoral zone when the water level increased to the highest level (104.4 m) in July (Figure 1). It is worth mentioning that the bank of the SW transect is gentle and soil slope and the banks of NE and SE transect are steep and rock slope. So vegetation could grow in the littoral zone of SW transect when the water level was low enough in spring. Such CH_4 emission peaks were also reported in the littoral zone of Miyun Reservoir and Three Gorges Reservoir (Yang et al., 2012, 2014).

Figure 10. The discharge flow in the downstream river below the dam at 9:00 a.m. during the measurement periods

The downstream CH_4 emissions (included the degassing at the turbines) are proportional to the streamflow in the previous studies (Fearnside and Pueyo, 2012). The degassing emissions at the turbines of Xing'anjiang Dam were not measured by the difference in CH_4 concentrations at the turbine intake and in the water below the

Biogeosciences Discuss., https://doi.org/10.5194/bg-2018-195
Manuscript under review for journal Biogeosciences
Discussion started: 3 May 2018
© Author(s) 2018. CC BY 4.0 License.

dam, because about the 500m upstream and downstream of the dam was forbidden to access to make sure the Xin'anjiang Dam safe. However, CH_4 emissions from the 4 sampling points, with the different distances to the dam, were measured 13 times in 2015 (Figures 7). The minimum value (0.19 ± 0.11 mg CH_4 m^{-2} h^{-1}) appeared in February, which was likely caused by the low the discharged flow (275 m^3 s^{-1}) at the downstream river during the measurement periods (Figure 10). Although the variability pattern of CH_4 emission was not completely consistent with the streamflow in the downstream river (Figures 7, 10), the streamflow below the dam still account for 25.3% seasonal variability of CH_4 emission in the DRP1 (Figure S3, $p<0.05$, $r=0.50$), which was about 500m downstream of the Xin'anjiang Dam.

4.2. Spatial Variations in CH_4 Emission

Figure 11. Schematic diagram of the spatiotemporal variability in CH_4 emission from Xin'anjiang Reservoir

The results were confirmed the hypothesis (2), with a high emission level in upstream and downstream river, and a low emission level in the main reservoir body (Figure 11). The obviously high CH_4 emission from the upstream river was contributed by the bubbles (Figures 3, 4, Table S2). However, few bubble was trapped in the floating chambers in the main body of the reservoir and the downstream river below the dam in 2015 (Figures 6, 7). The CH_4 ebullition fluxes in inflow rivers or upstream rivers were also reported in the many other reservoirs (DelSontro et al., 2011, Musenze et al., 2014; Beaulieu et al., 2014). Besides the bubble CH_4 fluxes, the diffusive CH_4 fluxes contributed to 30% of the total CH_4 flux there, and were more than 10 times and 2 times higher than those from the main body and the downstream river, respectively (Figure 8), which was attributed to the fast water velocity, shallow water depths, and a large amount of allochthonous carbon input. Water flow was fast in the upstream river during the heavy rainy days (especially in June), which carried plenty of allochthonous organic matter constantly. The deepest zone was about 20m in the NW transect, which was about half to one-third compared with the deepest sampling

Biogeosciences Discuss., https://doi.org/10.5194/bg-2018-195
Manuscript under review for journal Biogeosciences
Discussion started: 3 May 2018
© Author(s) 2018. CC BY 4.0 License.

421 points in the 3 transects of the main body. The shallow water depths would reduce the
422 transport path for small CH_4 molecule, and more CH_4 would reach the water-air
423 interface because the less amount of CH_4 was oxidized at the oxic layer by the
424 methanotrophic bacteria (Schubert et al., 2012).
425
426 **Table 1.** Previously reported CH_4 emission from temperate and subtropical reservoirs
427
428 The average CH_4 emission fluxes from the upstream river of Xin'anjiang Reservoir
429 were higher than that of Three Gorges Reservoir, China, Douglas Lake, USA, Nam
430 Theun 2 Reservoir, Laos, and Eguzon Reservoir, France, but lower than that in
431 William H. Harsha Lake, USA, Gold Creek and Little Nerang Reservoir, Australia
432 (Table 1). Diffusive CH_4 emission was measured from the upstream rivers of Three
433 Gorges Reservoir, Douglas Lake, Nam Theun 2 Reservoir, and Eguzon Reservoir,
434 because no bubble or a few bubbles were observed in the upstream rivers of the 4
435 reservoirs. A significant high CH_4 emission from the upstream river in Xin'anjiang
436 Reservoir contributed from bubbles, which was similar to the situations in the
437 upstream rivers of Harsha Lake, Gold Creek, and Little Nerang Reservoir.
438 Furthermore, The diffusive average CH_4 emission from the main body of Xin'anjiang
439 Reservoir (0.10 ± 0.07 mg $CH_4 \cdot m^{-2} \cdot h^{-1}$) was within the range of CH_4 emission level
440 reported in the other reservoirs in China (mean: 0.22 ± 0.18 mg $CH_4 \cdot m^{-2} \cdot h^{-1}$; Li et al.,
441 2015), but the CH_4 emission was 1-2 orders of magnitude lower than that from the
442 reservoirs in Australia and Laos (William H. Harsha Lake, Gold Creek Reservoir,
443 Little Narang Reservoir, Nam Leuk and Nam Theun 2 Reservoir), comparable to other
444 temperate or subtropical reservoirs listed in Table 1, except Douglas Lake and 5 small
445 reservoirs in Jiangxi Province, China.
446
447 Flooded barren soils, dendritic reservoir shape, and aerobic water body probably
448 caused the relative low CH_4 emission from the Xin'anjiang Reservoir. Before the
449 water storage of the Xin'anjiang Reservoir, strictly clearing activities were done under
450 the elevation of 70m. The left organic carbon would decompose in the first several

© Author(s) 2018. CC BY 4.0 License.

451 years after impoundment (Abril et al., 2005). After all, Xin'anjiang Reservoir was an
452 old reservoir with an age of 56-58 years, thus the remaining flooded organic carbon
453 had little contribution to CH_4 emission. Moreover, chlorophyll-a and water depth
454 controlled the reservoirs CH_4 emissions (Deemer et al., 2016). The ranges were in the
455 range of 1 to 3 μg/L for chlorophyll-a and 10 to 23 μg/L for total phosphorus in the
456 epilimnion of Xin'anjiang Reservoir, respectively (Li et al. 2011; Yu et al., 2010),
457 which was an oligotrophic reservoir, according to the classification standard of
458 nutrition for the tropical/subtropical reservoirs (Cunha et al., 2013). Besides, the
459 average water depth was about 34 m in the Xin'anjiang Reservoir, and the small CH_4
460 molecules were difficult to pass through such deep path. Furthermore, the Xin'anjiang
461 Reservoir was dendritic shape, so allochthonous organic carbon mainly deposited in
462 the sediments of NW lake (Yu et al., 1988, Figure 1), which had little contribution to
463 CH_4 emission from the main reservoir body. In addition, there was no anoxic layer in
464 Xin'anjiang Reservoir (Zhang et al., 2015), thus the methanotrophic bacteria could
465 oxidize the dissolve CH_4 at the aerobic conditions when they diffused to the
466 atmosphere (Yang et al., 2014b). All of these above factors combined together lead to
467 a relative low CH_4 emission flux in the reservoir's main body.
468
469 A significantly higher CH_4 emission was observed in the downstream river than that
470 in the water surfaces before the dam (Figure 8), which was probably released from the
471 dissolved CH_4 in reservoir's hypolimnions (Abril et al., 2005). Our data set did not
472 include the dissolved CH_4 concentration in different depths before the dam, but
473 previous related studies reported the dissolved CH_4 concentration increased with the
474 depth before the dam (Abril et al., 2005). The dissolved CH_4 would release to the
475 atmosphere because of the differences in pressure, temperature, and turbulence when
476 the water passed through the turbines and spillways (Yang et al., 2014b). Strong
477 turbulence made the dissolved CH_4 emission into the atmosphere in the downstream
478 river below the Xin'anjiang Dam. However, the diffusive CH_4 flux dropped with the
479 distances to the dam, with an obvious higher CH_4 flux in the DRP1 (Figure 9), which
480 was likely related to the decrease of turbulence strength with a distance to the dam

© Author(s) 2018. CC BY 4.0 License.

and the explosive release of CH_4 gas right after the turbines (degassing). The similar pattern of CH_4 emission was also observed in the downstream rivers of Balbina, Samuel, Petit-Saut, and Nam Theun 2 reservoirs, and CH_4 emission flux in 30 km was close to the natural rivers nearby (Kemenes et al., 2007; Deshmukh et al., 2016; Guérin et al., 2006).

5. Conclusion

The CH_4 fluxes data values obtained in Xin'anjiang Reservoir showed the its different seasonal variability: CH_4 emission from the main reservoir body had a high emission level in autumn, a low level in spring, and a similar medium levels in summer and winter; In the main upstream river of the reservoir, CH_4 emission was low in the first half year, but high in the second half year; CH_4 emission from the downstream river was largely influenced by the streamflow below the dam. In the spatial scale, CH_4 emission had a high emission level in the upstream river and downstream river, but a low emission level in the reservoir's main body. A thoroughly investigation should be carried out in the different reservoir regions for a long-term basis to discover the spatiotemporal variability in CH_4 emission flux in a hydroelectric reservoir system, which could avoid the error of estimating the CH_4 emission incorrectly. The rules on the temporal and spatial variability in CH_4 emission and its potential influencing variables would be helpful to take proper measures to reduce the greenhouse gases emissions from the hydroelectric reservoir system in terms of the reservoir's management.

Supplementary Materials:

Figure S1: Positive relationships between the ebullitive CH_4 emission and ebullition rates in the NW transect.

Figure S2. Positive relationship between the bubble CH_4 emission and bubble CH_4 concentration in the NW transect.

Figure S3. Positive relationship between the CH_4 flux value at DRP1 and streamflow.

Table S1. Complete dataset of the measured CH_4 emission fluxes by the floating chambers at the 3

© Author(s) 2018. CC BY 4.0 License.

511 sampling points of NW transect from Dec. 2014 to Jan. 2016.

512 Table S2. Complete dataset of the measured ebullitive CH_4 fluxs, ebullition rates, and CH_4
513 concentrations by the inverted funnels in the 26 sampling stations of the NW transect during Aug.
514 2016 to Nov. 2017.

515 Table S3. The measured CH_4 emission fluxes by the floating chambers at the 5 sampling points of
516 NE transect in 2015.

517 Table S4. Complete dataset of the measured CH_4 emission fluxes by the floating chambers at the 5
518 sampling points of SW transect from Dec. 2014 to Dec. 2015.

519 Table S5. Complete dataset of the measured CH_4 emission fluxes by the floating chambers at the 5
520 sampling points of SE transect from Jan. 2015 to Jan. 2016.

521 Table S6. Complete dataset of the measured CH_4 emission fluxes by the floating chambers at the 4
522 sampling points of downstream river from Dec. 2014 to Dec. 2015.

523

524 **Acknowledgements:** The study was funded by the National Natural Science
525 Foundation of China (41303065), the Project of Zhejiang Scientific and Technological
526 Plan (2015F30001) and Zhejiang Hangzhou Urban Forest Ecosystem Research
527 Station. We thank for the Xin'anjiang hydropower plant to provide the streamflow
528 data below the dam. Data presented in this work can be found in the supporting
529 information.

530

531 **Conflicts of Interest:** The authors declare no conflict of interest.

532

533 **References**

534 Abril, G., Guérin, F., Richard, S., Delmas, R., Galy-Lacauz, C., Gosse, P., Tremblay,
535 A., Varfalvy, L., Dos Santos, M., Matvienko, B.: Carbon dioxide and methane
536 emissions and the carbon budget of a 10-year old tropical reservoir (Petit Saut,
537 French Guiana), Global Biogeochem. Cy., *19*, GB4007, 2005.

538 Bastviken, D., Tranvik, L., Downing, J., Crill, P., Enrich-Prast, A.: Freshwater
539 methane emissions offset the continental carbon sink, Science, 50, 2011.

540 Beaulieu, J., Smolenski, R., Nietch, C., Townsent-Small, A., Elovitz, M.: High CH_4

© Author(s) 2018. CC BY 4.0 License.

emissions from a midlatitude reservoir draining an agricultural watershed. Environ. Sci. Technol., 48, 11100-11108, 2014.

Chanudet, V., Descloux, S., Harby, A., Sundt, H., Hansen, B., Brakstad, O., Serça, D., Guérin, F.: Gross CO_2 and CH_4 emissions from the Nam Ngum and Nam Leuk sub-tropical reservoirs in Lao PDR, Sci. Total Environ., 409, 5382-5391, 2011.

Cunha, D., Calijuri, M., Lamparelli, M.: A trophic state index for tropical/ subtropical reservoirs (TSI_{tsi}), Ecol. Eng., 60, 126-134, 2013.

Deemer, B., Harrison, J., Li, Y., Beaulieu, J., Delsontro, T., Barros, N., Bezerra-neto, J., Powers, S., Dos Santos, M., Arie Vionk, J.: Greenhouse gas emissions from reservoir water surfaces: a new global synthesis, Bioscience, 66, 949-964, 2016.

DelSontro, T., McGinnis, D., Sobek, S., OStrovsky, I., Wehrli, B.: Extreme methane emissions from a Swiss hydropower reservoir: Contribution from bubbling sediments, Environ. Sci. Technol., 44, 2419-2425, 2010.

DelSontro, T., Kunz, M., Kimpter, T., Wüest, A., Wehrli, B., Senn, D.: Spatial heterogeneity of methane ebullition in a large tropical reservoir, Environ. Sci. Technol., 45, 9866-9873, 2011.

DelSontro, T., Boutet, L., St-Pierre, A., Del Giorgio, P., Prairie, Y.: Methane ebullition and diffusion from northern ponds and lakes regulated by the interaction between temperature and system productivity, Limnol. Oceanogr., 61, S62-S77, 2016.

Descloux, S., Chanudet, V., Serça, V., Guérin, F.: Methane and nitrous oxide annual emissions from an old eutrophic temperature reservoir. Sci. Total Environ., 598, 959-972, 2017.

Deshmukh, C., Guérin, F., Labat, D., Pighini, S., Vongkhamsao, A., Guedant, P., Rode, W., Godon, A., Chanudet,V., Delscloux, S.: Serça D. Low methane (CH_4) emissions downstream of a monomictic subtropical hydroelectric reservoir (Nam Theun 2, Lao PDR), Biogeosciences, 13, 1919-1932, 2016.

Fearnside, P., Pueyo, S.: Greenhouse-gas emissions from tropical dams, Nat. Clim. Change, 2, 382-384, 2012.

Grinham, A., Dunbabin, M., Gale, D., Udy, J.: Quantification of ebullitive and atmosphere from a water storage, Atmos. Environ., 45, 7166-7173, 2011.

© Author(s) 2018. CC BY 4.0 License.

571 Guérin, F., Abril, G., Richard, S., Burban, B., Reynourd, C., Seyler, P., Delmas, R.:
572 Methane and carbon dioxide emissions from tropical reservoirs: significance of
573 downstream rivers, Geophys. Res. Lett., 33, L21407, 2006.
574 Guérin, F., Deshmukh, C., Labat, D., Pighini, S., Vongkhamsao, A., Guédant, P., Rode,
575 W., Godon, A., Chanudet, V., Descloux, S., Serça, D.: Effect of sporadic
576 destratification, seasonal overturn, and artificial mixing on CH_4 emissions from a
577 subtropical hydroelectric reservoir, Biogeosciences, 13, 3647-3663, 2016.
578 Hutchinson, G., Livingston, G.: Vents and seals in non-steady-state chambers used for
579 measuring gas exchange between soil and atmosphere, Eur. J. Soil Sci., 52, 675-682,
580 2001.
581 Jacinthe, P., Filippelli, G., Tedesco, L., Raftis, R.: Carbon storage and greenhouse
582 gases emission from a fluvial reservoir in an agricultural landscape, Catena, 94,
583 53-63, 2012.
584 Jiang, X., Zhang, L., Yao, X., Xu, H., Li, M.: Greenhouse gas flux at reservoirs of
585 Jiangxi Province and its influencing factors, J. Lake Sci., 29, 1000-1008, 2017.
586 Juutinen, S., Alm, J., Martikainen, P., Silvola, J.: Effect of spring flood and water
587 level drawn-down on methane dynamics in the littoral zone of boreal lakes,
588 Freshwater Bio., 46, 855-869, 2001.
589 Kemenes, A., Forsberg, B., Melack, J.: Methane release below a tropical hydroelectric
590 dam, Geophys. Res. Lett., 34, L12809, 2007.
591 Li, P., Shi, W., Liu, Q., Yu, Y., He, G., Chen, L., Ren, L., Hong, R.: Spatial and
592 temporal distribution patterns of chlorophyll-a and the correlation analysis with
593 environmental factors in Lake Qiandao, J. Lake Sci., 23, 568-574, 2011.
594 Li, Y., Zhang,Q., Bush, R., Sullivan, L.: Methane and CO_2 emission from China's
595 hydroelectric reservoirs: a new quantitative synthesis, Environ. Sci. Pollut. Res.,
596 *22*, 5325-5339, 2015.
597 Maeck, A., Hofmann, H., Lorke, A.: Pumping methane out of aquatic
598 sediments-ebullition forcing mechanisms in an impounded river, Biogeosciences,
599 11, 2925-2938, 2014.
600 Mendonça, R., Kosten, S., Sobek, S., Cole, J., Bastos, A., Albuquerque, A., Cardoso,

© Author(s) 2018. CC BY 4.0 License.

S., Roland, F.: Carbon sequestration in a large hydroelectric reservoir: an integrative seismic approach, Ecosystems, 17, 430-441, 2014.

Musenze, R., Grinham, A., Werner, U., Gale, D., Sturm, K., Udy, J., Yuan, Z.: Assessing the spatial and temporal variability of diffusive methane and nitrous oxide emissions from subtropical freshwater reservoirs, Environ. Sci. Technol., 48, 14499-14507, 2014.

Mosher, J., Fortner, A., Phillips, J., Bevelhimer, M., Stewart, A., Troia, M.: Spatial and temporal correlates of greenhouse gas diffusion from a hydropower reservoir in the southern United States, Water, 7, 5910-5927, 2015.

Natchimuthu, S., Sundgren, I., Gålfalk, M., Klemedtsson, L., Crill, P., Danielsson, A., Bastviekn, D.: Spatio-temporal variability of lake CH_4 fluxes and its influence on annual whole lake emission estimates, Limnol. Oceanogr., 61, S13-S26, 2016.

Ometto, J., Cimbleris, A., Dos Santos, M., Rosa, L., Abe, O., Tundisi, J., Stech, J., Barros, N., Roland, F.: Carbon emission as a function of energy generation in hydroelectric reservoirs in Brazilian dry tropical biome, Energ. Policy, 58, 109-116, 2013.

Rodriguez, M., Casper, P.: Greenhouse gas emissions from a semi-arid tropical reservoir in northeastern Brazil, Reg. Environ. Change, 18, 1-12, 2018.

Sobek, S., DelSontro, T., Wangfun, N., Wehrli, B.: Extreme organic carbon burial fuels intense methane bubbling in a temperate reservoir, Geophys. Res. Lett., 39, L01401, 2012.

Schubert, C., Diem, T., Eugster, W.: Methane emissions from a small wind shielded lake determined by eddy covariance, flux chambers, anchored funnels, and boundary model calculations: a comparison, Environ. Sci. Technol., 46, 4515-4522, 2012.

Soumis, N., Duchemin, E., Canuel, R., Lucotte, M.: Greenhouse gas emissions from reservoirs of the western United States, Global Biogeochem. Cy., *18*, GB3022, 2004.

Sturm, K., Yuan, Z., Gibbes, B., Grinham, A.: Methane and nitrous oxide sources and emissions in a subtropical freshwater reservoir, South East Queenland, Australia,

© Author(s) 2018. CC BY 4.0 License.

631 Biogeosciences, 11, 5245-5248, 2014.
632 Wang, X., He, Y., Yuan, X., Chen, H., Peng, C., Yue, J., Zhang, Q., Diao, Y., Liu, S.:
633 Greenhouse gases concentrations and fluxes from subtropical small reservoirs in
634 relation with watershed urbanization, Atmos. Environ., 154, 225-235, 2017.
635 Wik, M., Crill, P., Bastviken, D., Danielsson, A., Norbäck, E.: Bubbles trapped in
636 arctic lake ice: potential implications for methane emissions, J. Geophys. Res., 116,
637 G03044, 2011.
638 Wik, M., Crill, P., Varner, R., Bastviken, D.: Multiyear measurements of ebullitive
639 methane flux from three subarctic lakes, J. Geophys. Res., 118, 1307-1321, 2013.
640 Yang, M., Li, H., Ting, L., Zhou, Y., Lu, C., Li, L., Lei, G., Wang, J., Lu, X.:
641 Spatial-temporal characteristics of methane emission flux and its influence factors
642 at Miyun Reservoir in Beijing, Wetland Sci., 9, 191-197, 2011.
643 Yang, L., Lu, F., Wang, X., Duan, X., Song, W., Sun, B., Chen, S., Zhang, Q., Hou, P.,
644 Zheng, F., Zhang, Y., Zhou, X., Zhou, Y., Ouyang, Z.: Surface methane emissions
645 from different land use types during various water levels in three major drawdown
646 areas of the Three Gorges Reservoir, J. Geophys. Res., 117, 10109, 2012.
647 Yang, L., Lu, F., Wang, X., Duan, X., Song, W., Sun, B., Zhang, Q., Zhou, Y.: Spatial
648 and seasonal variability of diffusive methane emissions from the Three Gorges
649 Reservoir, J. Geophys. Res., 118, 471-481, 2013.
650 Yang, M., Geng, X., Grace, J., Lu, C., Zhu, Y., Zhou, Y., Lei, G.: Spatial and seasonal
651 CH_4 flux in the littoral zone of Miyun Reservoir near Beijing: the effects of water
652 level and its fluctuation, Plos one, 9, e94275, 2014a.
653 Yang, L., Lu, F., Zhou, X., Wang, X., Duan, X., Sun, B.: Progress in the studies on
654 greenhouse gas emissions from reservoirs, Acta Ecol. Sin., 34, 204-212, 2014b.
655 Yin, Y., Wu, Z., Liu, M., He, J., Yu, Z.: Dynamic distributions of dissolved oxygen in
656 lake Qiandaohu and its environmental influence factors, Environ. Sci., 35,
657 2539-2546, 2014.
658 Yu, Y. The Analysis of the deposits of the Xin'anjiang Reservoir (in Chinese with
659 English Abstract), J. East China Norm. Univ. (Nat. Sci.), 3, 77-84, 1988.
660 Yu, Y., Ren, L., Liu, Q., Shi, W., Liu, G., He, G., Chen, L., Hong, R.: Temporal and

© Author(s) 2018. CC BY 4.0 License.

661 spatial distribution of nutrients and influence factors of Lake Qiandao during
662 2007-2008, Wetland Sci., 22, 684-692, 2010.
663 Yang, L., Lu, F., Zhou, X., Wang, X., Duan, X., Sun, B.: Progress in the studies on
664 greenhouse gas emissions from reservoirs, Acta Ecol. Sin., 34, 204-212, 2014.
665 Zhang, Y., Wu, Z., Liu, M., He, J., Shi, K., Zhou, Y., Wang, M., Liu, X.: Dissolved
666 oxygen stratification and response to thermal structure and long-term climate
667 change in a large and deep subtropical reservoir (Lake Qiandaohu, China), Water
668 Res., 75, 249-258, 2015.
669 Zhao, Y., Wu, B., Zeng, Y.: Spatial and temporal patterns of greenhouse gas emissions
670 from Three Gorges Reservoir of China, Biogeosciences, 10, 1219-1230, 2013.
671 Zheng, H., Zhao, X., Zhao, T., Chen, F., Xu, W., Duan, X., Wang, X., Ouyang, Z.:
672 Spatial-temporal variations of methane emissions from the Ertan hydroelectric
673 reservoir in southwest China, Hydrol. Process., 25, 1391-1396, 2011.
674

Biogeosciences Discuss., https://doi.org/10.5194/bg-2018-195
Manuscript under review for journal Biogeosciences
Discussion started: 3 May 2018
© Author(s) 2018. CC BY 4.0 License.

675 # Figures List:

696

Biogeosciences Discuss., https://doi.org/10.5194/bg-2018-195
Manuscript under review for journal Biogeosciences
Discussion started: 3 May 2018
© Author(s) 2018. CC BY 4.0 License.

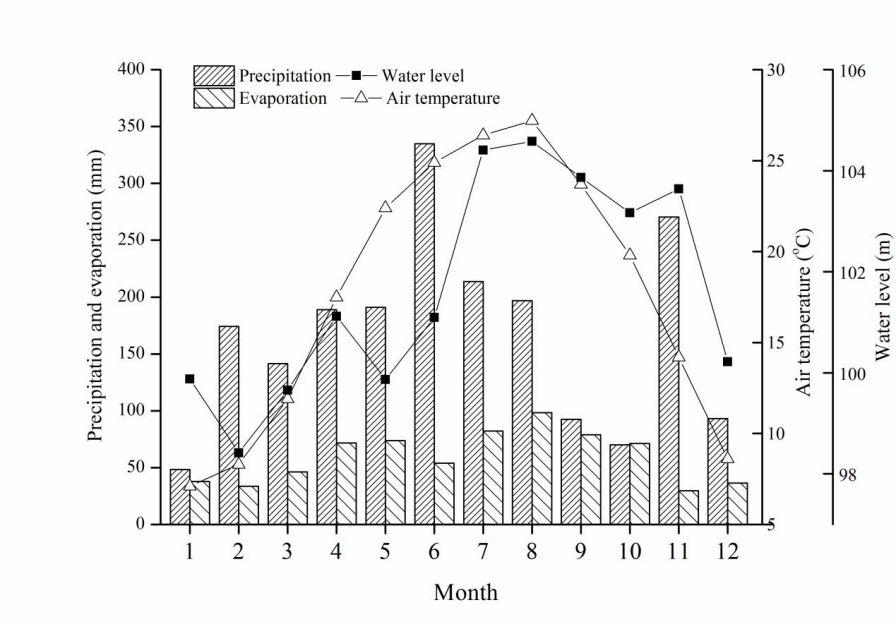

Figure 1

Biogeosciences Discuss., https://doi.org/10.5194/bg-2018-195
Manuscript under review for journal Biogeosciences
Discussion started: 3 May 2018
© Author(s) 2018. CC BY 4.0 License.

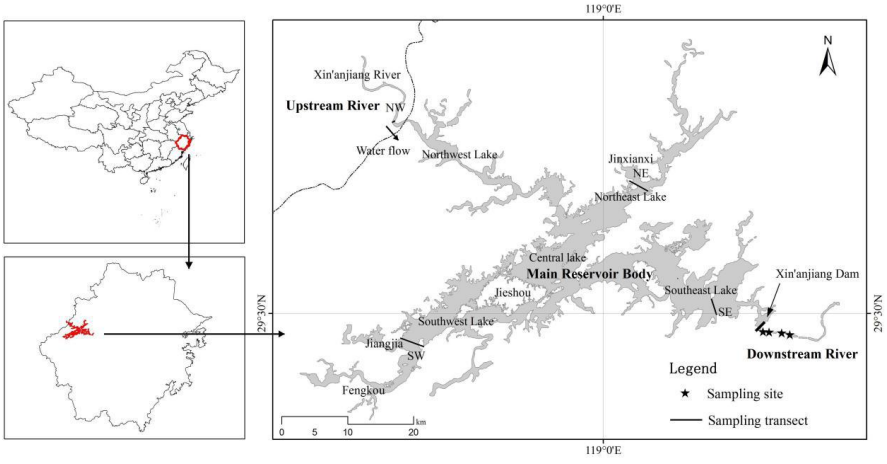

Figure 2

Biogeosciences Discuss., https://doi.org/10.5194/bg-2018-195
Manuscript under review for journal Biogeosciences
Discussion started: 3 May 2018
© Author(s) 2018. CC BY 4.0 License.

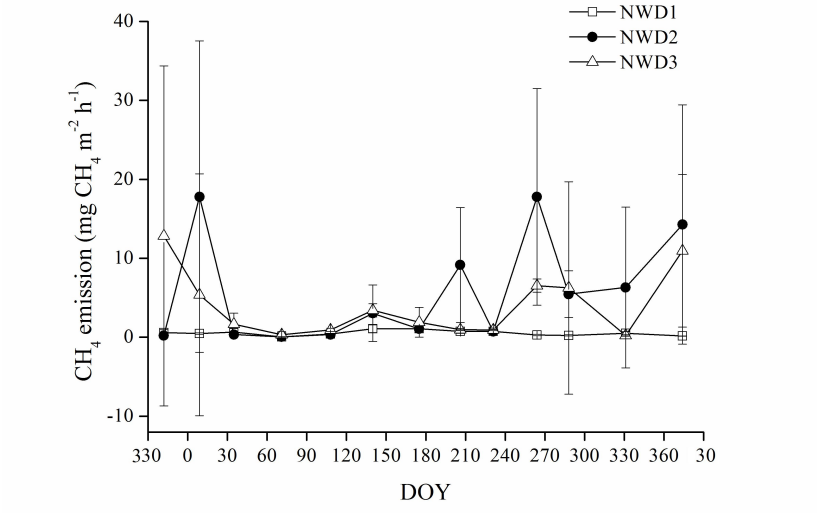

703

704 Figure 3

705

Biogeosciences Discuss., https://doi.org/10.5194/bg-2018-195
Manuscript under review for journal Biogeosciences
Discussion started: 3 May 2018
© Author(s) 2018. CC BY 4.0 License.

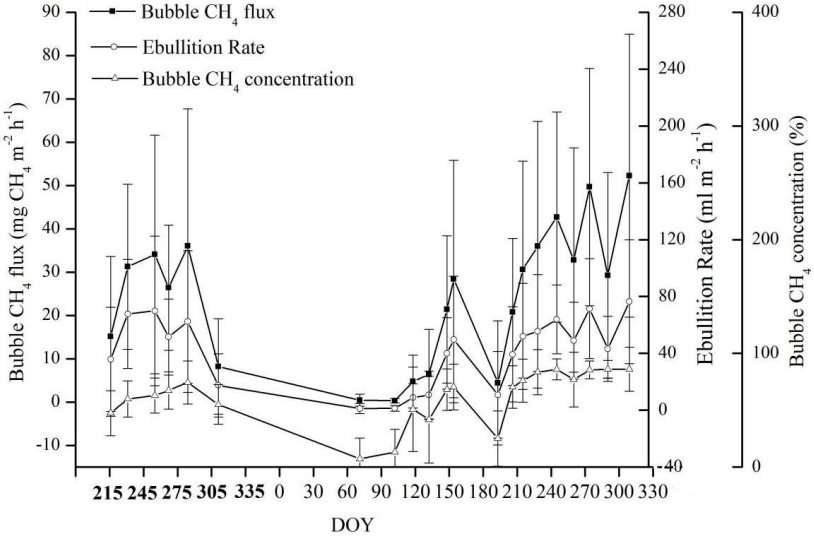

706

707 Figure 4

708

Biogeosciences Discuss., https://doi.org/10.5194/bg-2018-195
Manuscript under review for journal Biogeosciences
Discussion started: 3 May 2018
© Author(s) 2018. CC BY 4.0 License.

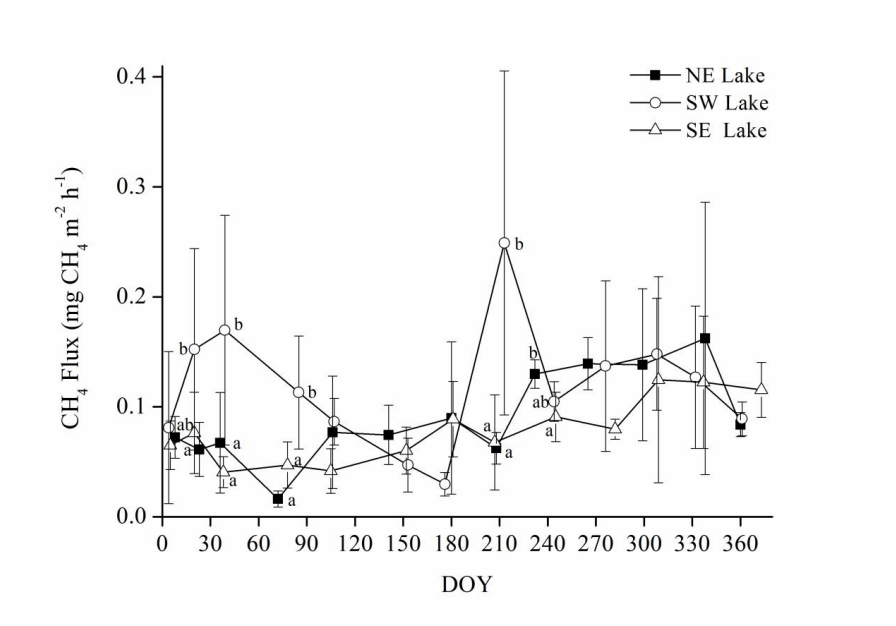

709

710 Figure 5

711

Biogeosciences Discuss., https://doi.org/10.5194/bg-2018-195
Manuscript under review for journal Biogeosciences
Discussion started: 3 May 2018
© Author(s) 2018. CC BY 4.0 License.

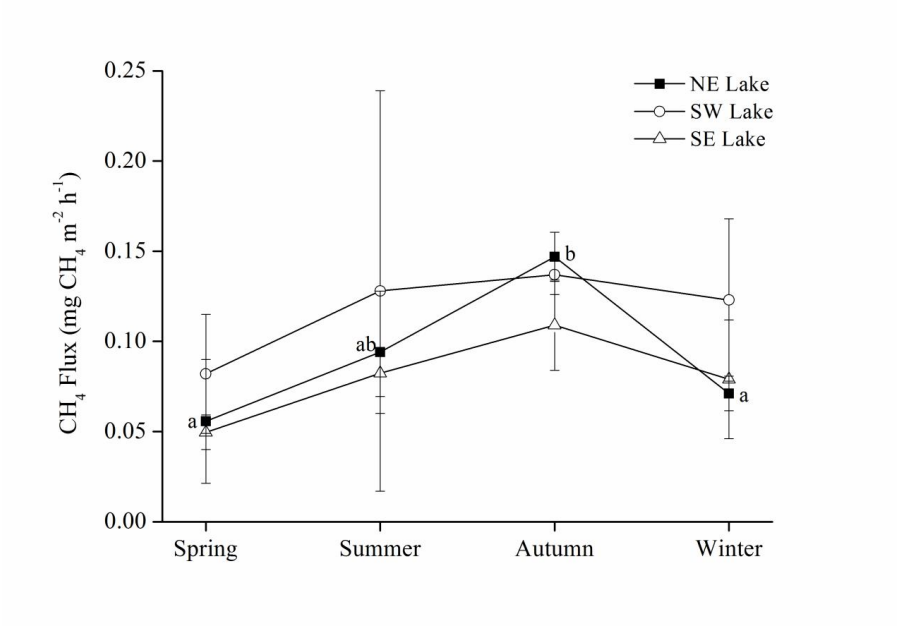

712

713 Figure 6

714

Biogeosciences Discuss., https://doi.org/10.5194/bg-2018-195
Manuscript under review for journal Biogeosciences
Discussion started: 3 May 2018
© Author(s) 2018. CC BY 4.0 License.

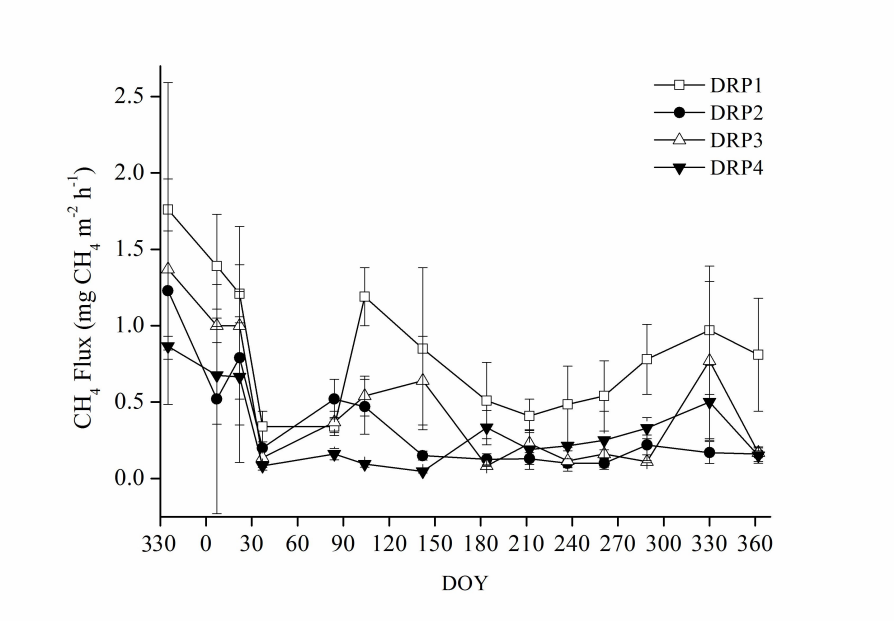

715

716 Figure 7

717

Biogeosciences Discuss., https://doi.org/10.5194/bg-2018-195
Manuscript under review for journal Biogeosciences
Discussion started: 3 May 2018
© Author(s) 2018. CC BY 4.0 License.

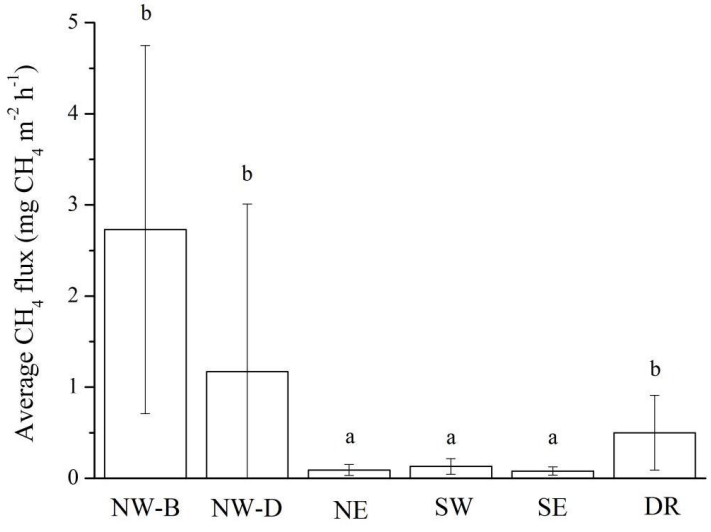

718
719 Figure 8
720

Biogeosciences Discuss., https://doi.org/10.5194/bg-2018-195
Manuscript under review for journal Biogeosciences
Discussion started: 3 May 2018
© Author(s) 2018. CC BY 4.0 License.

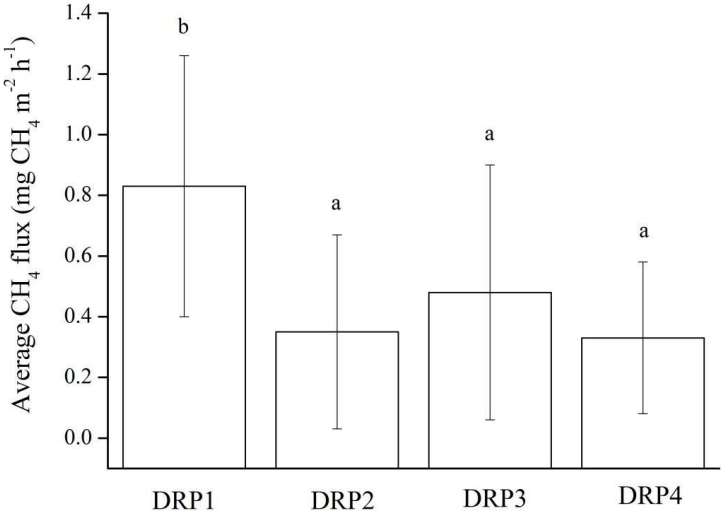

721

722 Figure 9

723

Biogeosciences Discuss., https://doi.org/10.5194/bg-2018-195
Manuscript under review for journal Biogeosciences
Discussion started: 3 May 2018
© Author(s) 2018. CC BY 4.0 License.

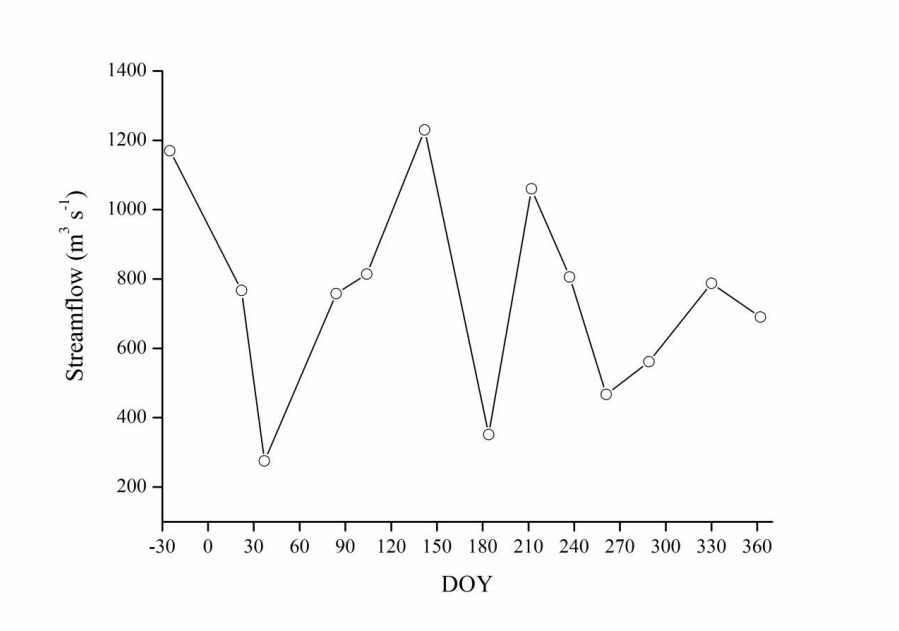

Figure 10

Biogeosciences Discuss., https://doi.org/10.5194/bg-2018-195
Manuscript under review for journal Biogeosciences
Discussion started: 3 May 2018
© Author(s) 2018. CC BY 4.0 License.

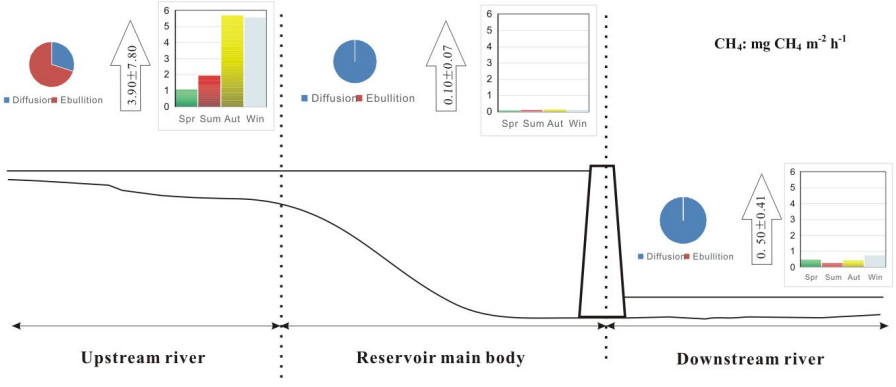

Figure 11

Biogeosciences Discuss., https://doi.org/10.5194/bg-2018-195
Manuscript under review for journal Biogeosciences
Discussion started: 3 May 2018
© Author(s) 2018. CC BY 4.0 License.

730 **Table 1. Previously reported CH_4 emission from temperate and subtropical reservoirs**

Country	Reservoir	CH_4 Flux (mg CH_4 m^{-2} h^{-1})			Refs
		Upstream river	Open water area	Downstream river	
China	Xin'anjiang	2.73 ± 2.02 (B) 1.17 ± 1.84 (D)	0.10 ± 0.07	0.50 ± 0.41	1
	Three Gorges	2.72 ± 1.98	0.23 ± 0.40	0.26 ± 0.16	2,3
	Ertan		0.12 ± 0.063		4
	Miyun		0.30 ± 0.31		5
	5 small reservoirs in Jiangxi Province		0.013 ± 0.01		6
	16 small reservoirs in Chongqing		0.63 ± 0.89		7
America	William H. Harsha Lake	130.72 ± 27.50	9.77 ± 2.00		8
	Douglas Lake	0.018 (D)	0.017 ± 0.012		9
	Eagle Creek		0.44 ± 0.73		10
	Six reservoirs in the Western US		0.13-0.40		11
Australia	Gold Creek	172.36 ± 24.72	12.35 ± 6.36		12
	Little Nerang Dam	247.03 ± 254.80	6.55 ± 16.83		13
Laos	Nam Leuk		1.68 ± 2.68		14
	Nam Ngum		0.13 ± 0.13		14
	Nam Theun 2	0.9-2.2	1.2-2.67	8.0 ± 14.7	15, 16
France	Eguzon	0.24 ± 0.56 (B) 2.2 ± 3.2 (D)	0.4 (0-2.67)	0.68 ± 0.68	17

731 Refs: 1. this study; 2. Zhao et al., 2013; 3. Yang et al., 2013; 4. Zheng et al., 2010; 5. Yang et al., 2011; 6. Jiang et
732 al., 2017; 7.Wang et al., 2017; 8. Beaulieu et al., 2014; 9. Mosher et al., 2015; 10. Jacinthe et al., 2012; 11. Soumis
733 et al., 2004; 12. Sturm et al., 2014; 13. Grinham et al., 2011; 14. Chanudet et al., 2011; 15. Guérin et al., 2016; 16.
734 Deshmukh et al., 2016; 17. Descloux et al., 2017. CH_4 Flux: B: Bubble emission; D: Diffusive emission.